Journal of Organometallic Chemistry 694 (2009) 1727–1735

Contents lists available at ScienceDirect

Journal of Organometallic Chemistry

journal homepage: www.elsevier.com/locate/jorganchem

An unexpected cluster opening upon the formation of electronically unsaturated η^3-(cyclooctenyl)metallacarboranes of rhodium(III) and iridium(III) with sterically reduced $[(PhCH_2)_2C_2B_9H_9]^{2-}$ ligand

Leonid S. Alekseev, Alexander V. Safronov, Fedor M. Dolgushin, Alexander A. Korlyukov, Ivan A. Godovikov, Igor T. Chizhevsky *

A. N. Nesmeyanov Institute of Organoelement Compounds of the RAS, 28 Vavilov Str., 119991 Moscow, Russian Federation

ARTICLE INFO

Article history:
Received 9 November 2008
Received in revised form 24 December 2008
Accepted 8 January 2009
Available online 14 January 2009

Keywords:
Closo- and *pseudocloso*-metallacarboranes of rhodium and iridium
Crystal structures
NMR spectroscopy
EXSY spectroscopy
DFT calculations
Bader's theory

ABSTRACT

The room-temperature metallation reactions of the K^+ salt of the [7,8-$(PhCH_2)_2$-7,8-*nido*-$C_2B_9H_{10}]^-$ anion (**1**) with the COD-metal μ-chloride dimers [$(\eta^4$-$C_8H_{12})_2Rh_2(\mu$-$Cl)_2$] (**2**) and [$(\eta^4$-$C_8H_{12})_2Ir_2(\mu$-$Cl)_2$] (**3**) in benzene/ethanol solution gave formally 16-electron *pseudocloso*-type complexes with the η^3-cyclooctenyl ligand at the metal vertices, [3-{(1–3-η^3)-C_8H_{13}}-1,2-$(PhCH_2)_2$-*pseudocloso*-3,1,2-$MC_2B_9H_9$] [**4**, M = Rh(III); **5**, M = Ir(III)]. No evidence supporting the existence of an agostic C–H···M bonding interaction in these compounds was obtained either from the crystallographic or the phase-sensitive 2-D [^{1}H–^{1}H] NOESY/EXSY studies of **4**. The extraordinary stability of complexes **4** and **5** can therefore be associated with their cage-deformed cluster structures, where electronically-deficient (16-electron) metal centers are believed to be stabilized by additional electron density released from the polyhedral C–C bond cleavage. DFT solid-state calculations performed for *closo* (18-electron) and *pseudocloso* (16-electron) Rh(III) complexes, [3-(η^5-C_5Me_5)-1,2-$(PhCH_2)_2$-*closo*-3,1,2-$RhC_2B_9H_9$] (**6**, C–C, 1.7397 Å) and [3-{(1–3-η^3)-C_8H_{13}}-1,2-(4′-$MeC_6H_4)_2$-*pseudocloso*-3,1,2-$RhC_2B_9H_9$] (**9**, C···C, 2.420(2) Å), showed that the electron density transfer from the carborane moiety to the rhodium center is marginally greater for complex **9**, in accordance with the idea that electronics rather than sterics play a crucial role in the stabilization of 16-electron *pseudocloso*-metallacarborane species.

© 2009 Elsevier B.V. All rights reserved.

1. Introduction

Twelve-vertex *pseudocloso*- [1] and *semipseudocloso*-metallacarboranes [2] of a unique open-cage architecture with broken or significantly strained polyhedral carbon–carbon connectivity have only lately been recognized as an important new subgroup of metallacarborane clusters, which geometrically lie intermediate between metallacarboranes of *closo* and *hypercloso/isocloso* structures on the Wade–Williams matrix [3]. These compounds due to rich structural chemistry as well as their potentiality for in-depth mechanistic study of the low-temperature polyhedral isomerization processes of icosahedral metallacarboranes have received increasing attention in recent years [4]. However, the vast majority of the known examples within this particular family are, at present, derived from either sterically encumbered *nido*-carboranes with arene substituents (mostly phenyl [3] or substituted phenyl groups [4f]) on the C_2B_3-pentagonal open face or from those *nido*-carboranes having electron rich alkyl- or arylheteroatom-containing substituents at the cage carbon atoms [4c–e], and among these, species possessing an 18-electron metal configuration are dominated.

Herein we report the synthesis, structural characterization and multinuclear NMR studies of the two novel 16-electron cage-deformed metallacarboranes derived from the C,C′-dibenzyl substituted [7,8-$(PhCH_2)_2$-7,8-$C_2B_9H_9]^{2-}$ carborane ligand, [3-{(1–3-η^3)-C_8H_{13}}-1,2-$(PhCH_2)_2$-*pseudocloso*-3,1,2-$MC_2B_9H_9$] (**4**, M = Rh(III); **5**, M = Ir(III)), in which electronically-deficient metal centers appear to be stabilized via partial opening of the cluster C–C connectivity rather than by a C–H···M agostic interaction. Also presented are the results of density functional theory (DFT) computations performed for two closely related to **4** and **5** species [3-(η^5-C_5Me_5)-1,2-$(PhCH_2)_2$-*closo*-3,1,2-$RhC_2B_9H_9$] (**6**) and [3-{(1–3-η^3)-C_8H_{13}}-1,2-(4′-$MeC_6H_4)_2$-*pseudocloso*-3,1,2-$RhC_2B_9H_9$] (**9**), whose 18-electron purely *closo* [5] and 16-electron *pseudocloso* [6] structures, respectively, have recently been crystallographically confirmed; these theoretical results corroborate the proposed mechanism of a metal stabilization in **4** and **5**.

* Corresponding author. Tel.: +7 495 1359334; fax: +7 495 1355085.
E-mail address: Chizbor@ineos.ac.ru (I.T. Chizhevsky).

0022-328X/$ - see front matter © 2009 Elsevier B.V. All rights reserved.
doi:10.1016/j.jorganchem.2009.01.014

2. Results and discussion

2.1. Synthesis and structural characterization of η^3-(cyclooctenyl)-pseudocloso-rhoda- (**4**) and η^3-(cyclooctenyl)-pseudocloso-iridacarborane (**5**) complexes

Previously, we have described a simple one-pot metallation procedure allowing to synthesize *closo*-rhoda- and *closo*-iridacarboranes with carbocyclic ligands of η^3-cycloallylic and $\eta^{3,2}$-cycloallylolefinic types in modest to high yields [7]. This approach proved to have broad versatility as a synthetic tool, and we have more recently applied a slightly modified method in the synthesis of a series of *pseudocloso*-(η-carbocycle)metallacarboranes having either a saturated 18-electron [4f] or an unsaturated 16-electron [6] configuration of a metal center. To further develop of this methodology, we now examined metallation reactions of the K^+ salt of the [7,8-$(PhCH_2)_2$-7,8-*nido*-$C_2B_9H_{10}]^-$ monoanion (**1**) with the related dimeric μ-chloride complexes [$(\eta^4$-$C_8H_{12})_2Rh_2(\mu$-$Cl)_2$] (**2**) and [$(\eta^4$-$C_8H_{12})_2Ir_2(\mu$-$Cl)_2$] (**3**). The reactions have been found to proceed at room temperature in a benzene–ethanol mixture (4:1) to produce the η^3-cyclooctenyl-type complexes **4** or **5** as sole products which, after column chromatography, were isolated as analytically pure orange crystalline solids in 47% and 95% yield, respectively (Scheme 1). The yield of rhodacarborane **4** can be improved up to 94% by carrying the reaction of K^+ salt of **1** with the reagent **2** under gentle heating in benzene at 60 °C.

Examination of the literature revealed that examples of metallacarborane clusters derived from the carborane system [*nido*-7,*n*-$C_2B_9H_{12}]^-$ (*n* = 8 or 9) having benzyl substituents at the cage carbon atoms are scarce, and only complexes with group IV metals [8] and early lanthanides [9] have been reported hitherto and structurally characterized. Interestingly, these C,C′-dibenzyl-substituted metallacarborane were found to adopt either "heavily slipped" *closo* or *exo-nido* structures, but not the purely *closo* structure as might, in principle, be expected due to the presence of spacer methylene groups in the relatively bulky benzyl substituents. Although the above examples [8,9] marginally confirmed that benzyl substituents are able to function as sterically demanding groups, our most recent work on the synthesis of complex [3-(η^5-C_5Me_5)-1,2-$(PhCH_2)_2$-*closo*-3,1,2-$RhC_2B_9H_9$] (**6**), has shown that these groups, although being somewhat bulky, may not always be located in close proximity to the capping metal-containing fragment to cause strong intramolecular steric crowding in 12-vertex metallacarborane *closo* systems [5]. It seemed probable, therefore, that to cleave the cluster carbon–carbon connectivity in complexes **4** and **5** with opening of their *closo* structures, no serious intramolecular steric crowding would occur due to benzyl substituents at the cage carbon atoms.

In order to unambiguously elucidate the detailed cluster structures, both complexes **4** and **5** were studied by single-crystal X-ray diffraction. The crystal structures of both species proved to have two independent molecules, which show only small differences in their bond distances and angles (selected values are listed in Table 1); the molecular structure of only one of them in each case is therefore shown in Fig. 1. The η^3-cyclooctenyl ligand in both **4** and **5** is essentially symmetrically bound to the metal atom, the average M–C(01) and M–C(03) separation being almost identical in the two species: (**4**, M = Rh, 2.184(4) and 2.181(4) Å) and (**5**, M = Ir, 2.177(8) and 2.183(8) Å). Both structures possess a non-crystallographic pseudomirror plane symmetry passing through the M(3), C(02), C(06), B(8), B(10), and B(6) atoms, thus rendering the two halves of each molecule equivalent. The distances between the metal center and the aliphatic CH_2 groups adjacent to the allyl unit, which might be expected to be involved in the C–H···M agostic interaction, proved to be very close to each other with the shortest average distance in complex **4** (Rh···C(08), 2.935(4) Å) being out of the range 2.6–2.7 Å, the distances typically observed for agostic η^3-cyclooctenyl-type complexes of transition metals [10].

Rather to our surprise, the cluster geometries of both **4** and **5** proved to be substantially distorted. Of particular importance is that both structures **4** and **5** have the tetragonal open face C(1)M(3)C(2)B(6), which is resulted from breaking of the C(1)–C(2) cluster connectivity. The average separations between the cage carbon atoms C(1)···C(2) and the contracted M(3)···B(6) interatomic distance for two independent molecules of **4** are 2.22 and 3.12 Å; the corresponding separations in **5** are 2.32 and 3.05 Å, respectively (Table 1). Thus, the observed structural cage-deformed characteristics of **4** are comparable with those of *semi-pseudocloso*-metallacarboranes [2,3], and those of complex **5** fit better with *pseudocloso*-shaped systems [1,3].

Interestingly, the cage C···C distance in the earlier reported complex [3-{(1–3-η^3)-C_8H_{13}}-1,2-$(CH_3)_2$-3,1,2-*closo*-$RhC_2B_9H_9$] (**7**) [11] that contains less bulky C,C′-dimethyl substituents is in fact lengthened only to 1.851 Å [11], whereas the corresponding distances in the related C,C′-diphenyl- and C,C′-di(*p*-tolyl)-substituted compounds [3-{(1–3-η^3)-C_8H_{13}}-1,2-Ar_2-3,1,2-*pseudocloso*-$MC_2B_9H_9$] (**8**, M = Rh, Ar = Ph [3]; **9**, M = Rh, Ar = 4′-MeC_6H_4 [6]; **10**, M = Ir, Ar = 4′-MeC_6H_4 [6]) are increased significantly up to 2.410, 2.420, and 2.438 Å, respectively, so that they are no longer regarded as a bonding interaction. The C···C separation found in **8**–**10** may be compared with those observed in the closely related 16-electron species [3-{(1–3-η^3)-C_8H_{13}}-1-SPh-2-Ph-3,1,2-*pseudocloso*-$RhC_2B_9H_9$] (**11**) (2.427 Å) [12], wherein the thiophenyl group with the sulphur lone electron pair and the phenyl group at the cage carbons may exert the cumulated electronic and steric effects to assist a polyhedral C···C elongation [4e]. In the case of electron-deficient complexes **4** and **5**, the steric effect brought about by two cage-bound benzyl C,C′-substituents, although cannot be fully discounted, appeared to be not the major factor responsible for C–C cleavage in their crystal structures (*vide infra*).

2.2. Comparative NMR spectroscopic examination of pseudocloso complexes **4** and **5** and other related compounds with or without agostic (C–H···M) bonding interaction

The unique stability, both in the solid state and in solution, of all the above-considered 16-electron Rh(III) and Ir(III) *closo*- or

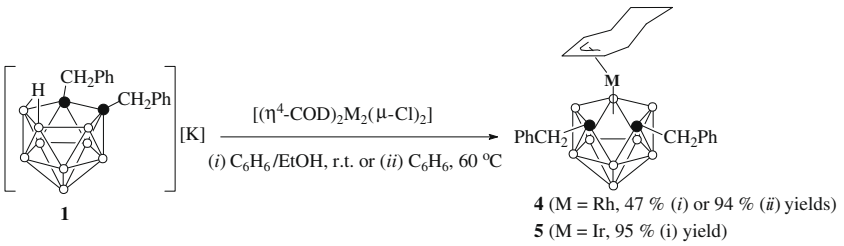

Scheme 1.

Table 1
Selected bond lengths (Å) and angles (°) for two independent molecules of **4** and **5**.

	4 (M = Rh)		**5 (M = Ir)**	
	A	B	A	B
M(3)–C(1)	2.140(4)	2.144(3)	2.144(8)	2.137(7)
M(3)–C(2)	2.133(4)	2.130(4)	2.108(8)	2.133(8)
M(3)–B(4)	2.194(5)	2.210(4)	2.205(10)	2.210(10)
M(3)–B(7)	2.213(4)	2.208(4)	2.216(10)	2.203(9)
M(3)–B(8)	2.113(4)	2.092(4)	2.144(10)	2.100(8)
M(3)–C(01)	2.190(4)	2.178(4)	2.187(9)	2.166(7)
M(3)–C(02)	2.144(4)	2.145(4)	2.141(9)	2.146(7)
M(3)–C(03)	2.176(4)	2.185(4)	2.166(8)	2.199(8)
M(3)···C(04)	2.919(4)	2.969(4)	2.947(9)	2.974(8)
M(3)···C(08)	2.941(4)	2.929(4)	2.926(8)	2.966(8)
M(3)···B(6)	3.127(4)	3.107(4)	3.047(9)	3.045(9)
C(1)···C(2)	2.200(6)	2.235(6)	2.340(11)	2.299(13)
C(01)–C(02)	1.416(5)	1.410(5)	1.421(12)	1.391(10)
C(01)–C(08)	1.503(5)	1.519(5)	1.494(12)	1.526(10)
C(02)–C(03)	1.406(6)	1.404(6)	1.402(13)	1.433(11)
C(03)–C(04)	1.518(6)	1.522(6)	1.489(12)	1.484(10)
C(04)–C(05)	1.544(6)	1.545(6)	1.535(12)	1.558(13)
C(05)–C(06)	1.506(6)	1.515(7)	1.484(13)	1.503(14)
C(06)–C(07)	1.525(5)	1.541(6)	1.492(10)	1.496(12)
C(07)–C(08)	1.540(5)	1.542(5)	1.518(11)	1.556(10)
C(1)–M(3)–C(2)	62.0(2)	63.1(2)	66.8(3)	65.1(4)
M(3)–C(1)–C(6)	107.6(3)	106.2(3)	101.7(5)	103.9(5)
M(3)–C(2)–C(6)	107.9(2)	106.9(2)	104.5(5)	104.0(5)
C(1)–B(6)–C(2)	79.3(3)	80.6(3)	83.7(5)	84.1(5)
C(02)–C(01)–C(08)	124.8(3)	124.8(3)	121.9(8)	124.7(7)
C(03)–C(02)–C(01)	122.6(4)	122.4(4)	122.3(8)	121.8(7)
C(02)–C(03)–C(04)	124.8(4)	126.0(3)	124.7(8)	124.8(8)
C(03)–C(04)–C(05)	114.4(4)	113.7(3)	114.2(9)	114.3(8)
C(06)–C(05)–C(04)	116.7(4)	117.4(4)	118.5(8)	116.7(8)
C(05)–C(06)–C(07)	116.3(4)	116.0(4)	115.7(9)	117.2(9)
C(06)–C(07)–C(08)	118.9(3)	117.8(3)	118.5(8)	118.6(7)
C(01)–C(08)–C(07)	114.8(3)	114.5(3)	116.6(8)	113.5(7)
C(14)–C(13)–C(1)	118.1(3)	114.6(3)	118.0(6)	114.5(6)
C(21)–C(20)–C(2)	118.0(3)	117.0(3)	118.9(6)	117.3(7)

pseudocloso-metallacarboranes is another important question. Presumably, their stability is increased not only due to the presence of electron-donating cage substituents, such as methyl groups in C,C′-dimethylated complex **7** [11], or benzyl groups in complexes **4** and **5**, but also might be due to a C–H···M agostic interaction, if it exists in these complexes in solution. With this in mind, compounds **4** and **5** were carefully examined, first with the aid of the conventional NMR spectroscopic methods.

The room-temperature ^{1}H NMR spectrum of **4** displays a set of two resonances at δ 5.73 (q, H(1,3)) and 4.76 (t, H(2)) ppm of relative intensity of 2:1, respectively, which can be assigned to the η^3-allyl unit of the carbocyclic C_8-ring ligand. This is in agreement with the $^{13}C\{^1H\}$ NMR spectrum of **4**, where the characteristic ^{103}Rh-coupled doublets were observed at δ 108.4 (J(Rh,C) = 5.7 Hz, C(2)) and 84.1 ppm (J(Rh,C) = 7.8 Hz, C(1,3)). Both these observations are entirely consistent with the metallacarborane species bearing the η^3-cyclooctenyl ligand at the rhodium vertex. The 2D [^{1}H–^{13}C]-HETCOR correlation spectrum of **4** showed that each pair of *exo* and *endo* protons at C(4), C(8) and C(5), C(7), respectively, appears as single 2H multiplets in the typical aliphatic region of the spectrum, at δ from 1.1 to 2.7 ppm. In the $^{13}C\{^1H\}$ NMR spectrum of **4**, each pair of the aforementioned carbon atoms including those of the cluster carbons, as well as all parent signals from two benzyl substituents, are also observed as equivalent. Analysis of both the ^{1}H and $^{13}C\{^1H\}$ NMR spectra of **5** showed that they are similar in many details to those of **4** with an exception that the resonances of the allylic portion of the η^3-C_8H_{13} ligand in the ^{1}H NMR spectrum of **5** are less resolved and are observed as separate signals at δ 5.42 (q, H(1,3)) and 5.38 (br m, H(2)) ppm only at low temperature, down to −30 °C. The $^{11}B\{^1H\}$ NMR spectra of **4** and **5** both display a set of six resonances with a 1:1:2:2:2:1 intensity ratio, as can be expected due to their symmetrical structures. Interestingly, complexes **4** and **5** are characterized by rather unexpected weighted average ^{11}B chemical shifts <δ(^{11}B)> at −2.67 and −1.10 ppm, respectively, whilst for the known *semipseudocloso*- and *pseudocloso*-metallacarboranes with an 18-electron metal configuration these are usually ranging between 0 and +6 ppm [3] with the only exception for [3-(η^6-Ar)-1,2-$(PhS)_2$-3,1,2-*semipseudocloso*-$RuC_2B_9H_9$] (Ar = *p*-cymene), where it is −2.2 ppm [4c]. Thus, all conventional multinuclear NMR data indicate that species **4** and **5** both display either "static" non-agostic (16-electron) structures or the existence in the molecules of the agostic C–H···M bonding interaction exhibiting rapid exchange between two *endo* C–H bonds adjacent to the allyl moiety of the C_8-ring.

In view of possible agostic structure of **4**, it is of significance to compare the ^{1}H NMR shielding patterns observed for **4** to those of other known η^3-(cyclooctenyl)rhodacarborane complexes **7**, **9**, **12**, and **13** whose agostic or non-agostic structures have been firmly confirmed either by single-crystal X-ray diffraction or by carefully performed multinuclear NMR spectroscopic studies. Some of the results of such spectroscopic comparison are presented in Fig. 2. It can be seen that *ortho*-xylylene-substituted compound [3-{(1–3-η^3)-C_8H_{13}}-1,2-μ-(*ortho*-xylylene)-3,1,2-*closo*-$RhC_2B_9H_9$] (**12**) is the only rhodium species of this series that displays the unique resonance in the nagative zone of the spectrum (δ –0.25 ppm)

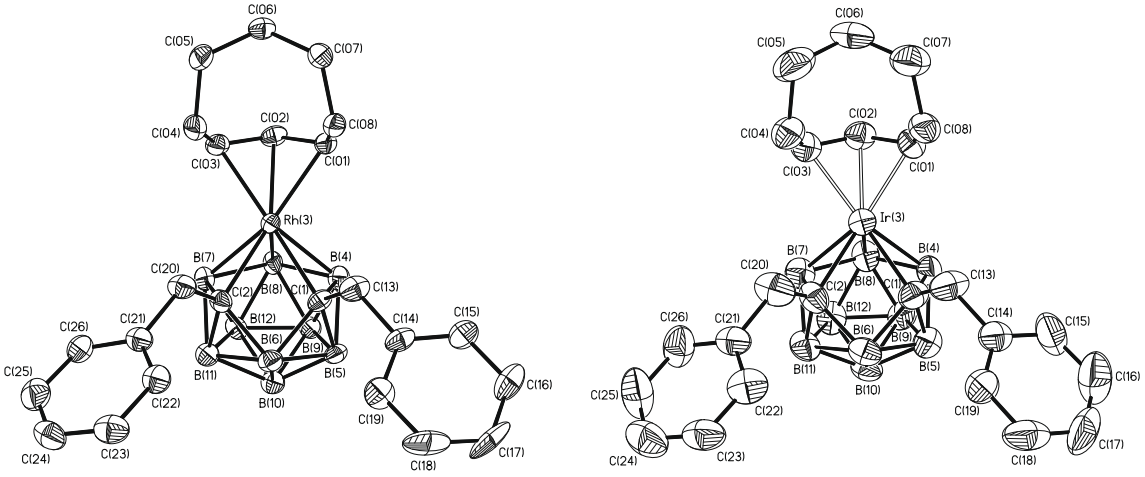

Fig. 1. ORTEP representations of the molecular structures of complexes **4** (left) and **5** (right), with thermal ellipsoids drawn at the 30% probability level. The hydrogen atoms are omitted for clarity. One of the two independent molecules for each complex is shown.

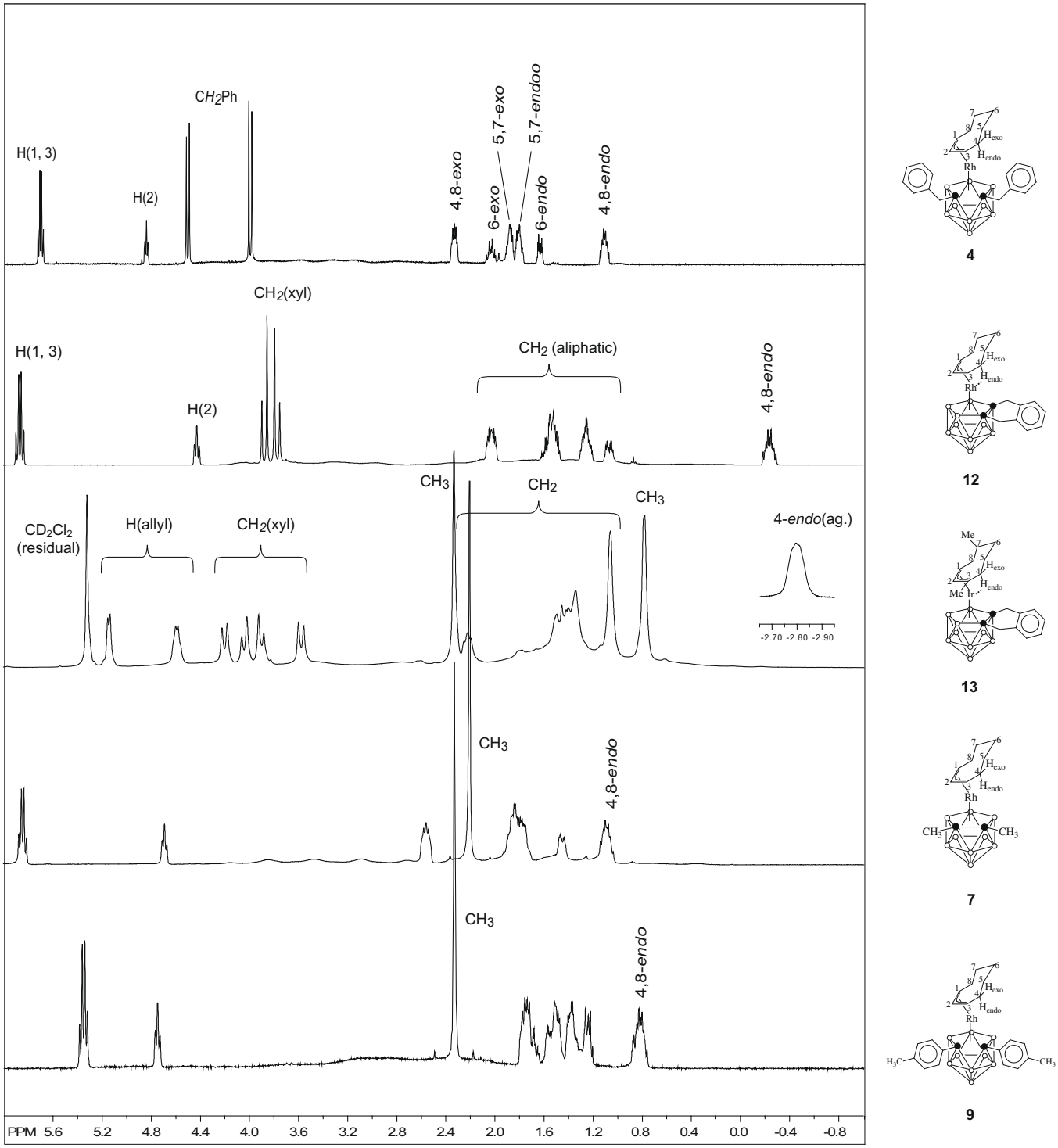

Fig. 2. 400 MHz ^{1}H NMR spectra of complexes **4**, **7**, **9** and **12** in $CDCl_3$ (22 °C), as well as **13** in CD_2Cl_2 (−73 °C) [14]), showing the assignment of proton resonances (aromatic region is not shown).

which could thus reasonably be attributed to an agostic (C–H···Rh) hydrogen involved in a rapid exchange between the two *endo* hydrogen atoms H(4) and H(8) of the C_8-ring. Indeed, this last complex, on the basis of multinuclear NMR spectroscopic data combined with the 2D [^{1}H–^{1}H]-EXSY experiments, has recently been assigned as having the fluxional agostic structure [13]. It can also be seen that there is a close relationship in the negative shift of an agostic hydrogen between complex **12** and [3-{(1–3-η^3)-(1,5-$Me_2C_8H_{11}$}-1,2-μ-(*ortho*-xylylene)-3,1,2-*closo*-$IrC_2B_9H_9$] (**13**) which is known to have a "static" agostic structure at low temperature (−73 °C) [14]. Interestingly, all other C,C′-disubstituted rhodacarborane complexes of this series, including complex **4**, exhibit positive chemical shifts for the *endo*-H(4,8) resonances which might be possibly involved in the agostic interaction in each of these species. This fact might perhaps tend to support the idea that no agostic bonding interaction occurs among compounds **4**,

7, and **9**. However, the study of fluxional behavior in solution of complex **4** compared with **7**, **9** and **12** using the phase sensitive 2D [^{1}H–^{1}H] NOESY/EXSY correlation spectroscopy has shown that the above postulation to be the case only for complexes **4** and **9** which have *pseudocloso* cluster structure.

2.3. Dynamic properties in solution of closo and pseudocloso η^3-(cyclooctenyl)rhodacarborane complexes. Comparative examination using the phase sensitive 2D [^{1}H–^{1}H]-EXSY correlation spectroscopy

It has previously been demonstrated [13] that such a 2D correlation technique proved to be extremely useful tool in the analysis and identification of the fluxional agostic (C–H···Rh) complex **12**. In the work that we now report, we have applied the same exchange NMR technique for the comparable study of two earlier reported species **7** [11] and **9** [6] that are closely related to **4** and **5**. In both complexes **7** and **9** in solution no C–H···Rh agostic bond was earlier found by NMR spectroscopy, hence the Rh(III) atom in these molecules has been postulated to have 16-electron rather than 18-electron configuration.

The room-temperature 2D [^{1}H–^{1}H]-NOESY/EXSY correlation experiments were first carried out for *closo* complex **7**, and the result obtained appeared to be rather unexpected. The room-temperature 2D [^{1}H–^{1}H]-EXSY spectrum of the ostensibly non-agostic complex **7** revealed full identity with that of the agostic *closo* species **12**, earlier examined by the same NMR method at 60 °C [13] and now, for comparison with **7**, at room temperature. Both spectra shown in Fig. 3 were indicative of species undergoing rapid alternating of the C–H···Rh interactions in which all five *endo*-hydrogens including those at C(4) and C(8) are involved in mutual exchange; in addition, all the exchange cross-peaks between resonances of allyl and *exo* hydrogens of the C_8-ring have also been found in the spectra. These data provided the convincing evidence for the existence of an agostic C–H···Rh interaction in *closo* complex **7** in solution. In contrast to **7** and **12**, we have not succeeded in obtaining the room-temperature 2D [^{1}H–^{1}H]-EXSY spectra for complexes **4** and **9**; instead, the 2D [^{1}H–^{1}H]-NOESY spectra with negative off-diagonal cross-peaks were observed. The failure to detect any intramolecular exchange in solution of complexes **4** and **9** suggests their probable "static" solution structures. In a more general context, this fact leads to the conclusion that the agostic interaction in both species **4** or **9**, if it is still occurring in solution, should be termed as an extremely weak interaction, may be "pre-agostic", at maximum. In fact, such a weak C–H···Rh interaction would have a negligible influence on the stabilization of electronically-deficient metal center in these molecules.

On the basis of these results, two possible alternative mechanisms of stabilization of a formal 16-electron metal center in the η^3-cyclooctenyl metallacarboranes may be suggested. In complexes that are based on the tethered {*nido*-$R_2C_2B_9$} carboranes, where the cage carbon atoms are compactly held together as in **13** (C–C, 1.641 Å [14]), the agostic C–H···M interaction should be expected to play the crucial role in stabilizing of electronically-deficient metal centers. In complexes that contain sterically demanding carborane ligands, which generally lead to *pseudocloso- or semipseudocloso*-type metallacarborane structures with broken or significantly strained C···C polyhedral connectivity, a 16-electron metal center may be stabilized via its interaction with an electron density released from the cleavage of a polyhedral C–C bond. We believe, such stabilization occurs in complexes **4** and **5**, as well as, **9** and **10**. However, there may be intermediate cases, when the cage C,C′-substituents are insufficient for the complete cleavage of the skeletal C–C bond due to their limited steric effect. Additional electrons required for stabilization of an unsaturated metal center, in these cases, would most likely be provided by a combined mechanism. Based on this mechanism, electrons of the lengthened or partially broken polyhedral C–C bond, as well as electrons supplied to the metal center via the agostic C–H···M interaction, are simultaneously involved in such stabilization. Stabilization of electronically-deficient metal center

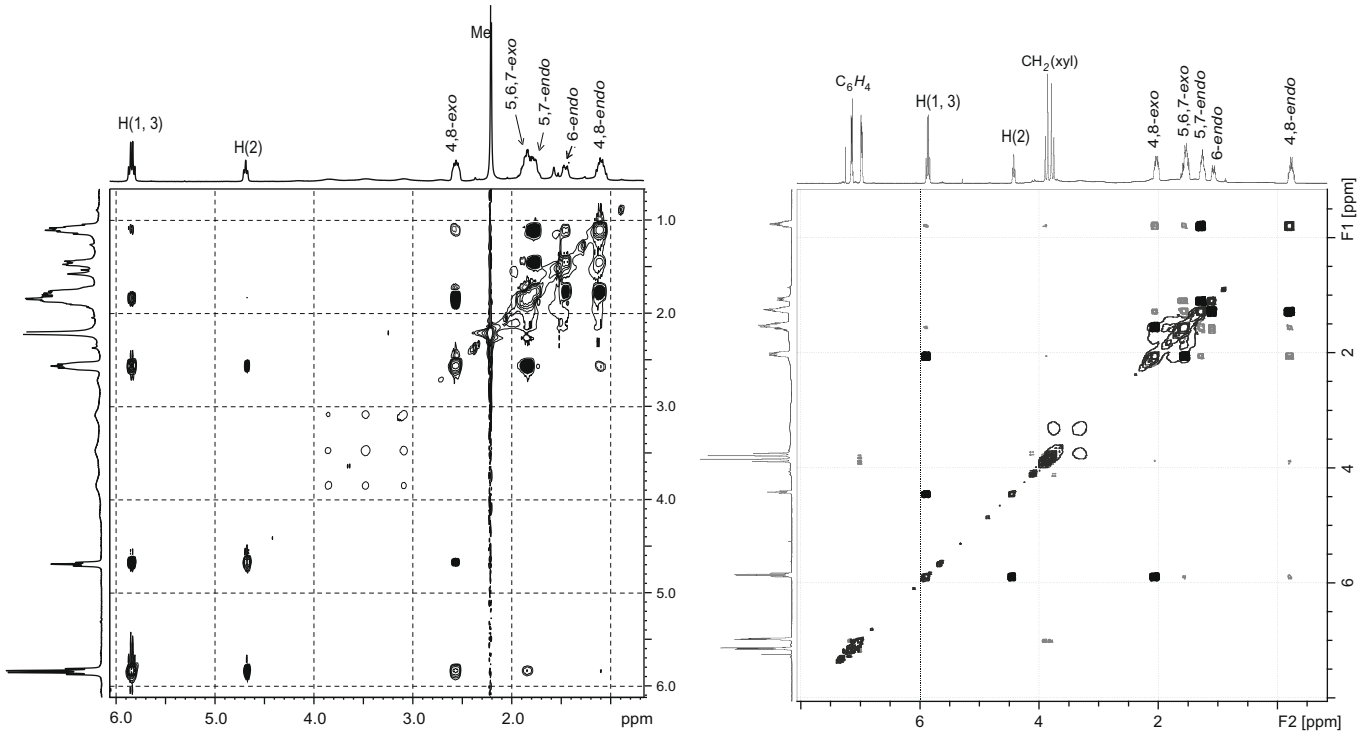

Fig. 3. The phase sensitive 2D [^{1}H–^{1}H]-EXSY spectra of **7** (left) and **12** (right) at the room temperature. The spectra were phased such that the positive off-diagonal cross-peaks are indicative of chemical exchange (marked as black spots in the figures).

in agostic complex **7** could likely proceed via this particular scheme.

2.4. Comparative computational studies and topological analysis of 16-electron closo- and 18-electron pseudocloso-type models of C,C′-disubstituted rhodacarboranes with the bulky cage substituents

To further confirm the proposed stabilization mechanism in *pseudocloso*-type metallacarborane complexes, solid-state DFT calculations [15] were performed for the two alternative Rh(III) complexes **6** and **9**, used as models of *closo* (18-electron) and *pseudocloso* (16-electron) metallacarboranes with the closely related bulky cage substituents. It should be noted that, according to X-ray diffraction data, the crystal structures of both complexes **6** [5] and **9** [6] have only one independent molecule each, rather than two crystallographically independent molecules in the case of **4** and **5**, and due to this fact complexes **6** and **9** are more suitable for computational studies.

Optimized crystal structures of **6** and **9** reproduced the experimental ones with sufficient accuracy. The discrepancies between experimental and calculated Rh–C and Rh–B distances do not exceed 0.02 Å (Table 2). The most pronounced differences (0.03–0.1 Å) are observed in the case of intermolecular H···H distances. Thus the electron structure of **6** and **9** calculated by DFT method is a good model for investigation of chemical bonding pattern in a coordination polyhedron of the Rh(III) atom. In order to study the electronic structure of **6** and **9** we have utilized R. F. Bader's theory "Atoms in molecules" (AIM) [18] which is based on the topological analysis of electron density distribution function ($\rho(r)$). Previously, we successfully used this approach for investigations of the 12-vertex Ph-substituted *ortho*-carboranes [19]. In this paper, we have focused on analysis of occupancies of atomic basins (AIM charges), whose values, we believe, can be indicative of rearrangement of electron density in the Rh(III) atom coordination polyhedron area.

Topological analysis of calculated $\rho(r)$ has shown the presence of critical points CP(3,-1) in the regions of all coordination Rh–C and Rh–B bonds. All these Rh–C and Rh–B bonds are characterized by positive values of laplacian of $\rho(r)$ ($\nabla^2\rho(r)$) and negative values of local energy density ($E^e(r)$) in CP(3,-1) that correspond to the intermediate type of interatomic interactions in terms of AIM theory (Table 3). On the contrary, the CP(3,-1) corresponding to B–B and C–B bonds in carborane cages, as well as C–C and C–H bonds in the η^5-Cp^* and η^3-C_8H_{13} ligands in both **6** and **9** have negative values of $\nabla^2\rho(r)$ and $E^e(r)$. A number of H···H closed-shell intermolecular interactions (positive sign of $\nabla^2\rho(r)$ and $E^e(r)$ in CP(3,-1)) have also been found. The topological characteristics of C(1)–C(2) bond in **6** (e.g. values of $\rho(r)$, $\nabla^2\rho(r)$ and $E^e(r)$) are similar to those found in the 12-vertex C-phenylated *ortho*-carboranes [19]. In contrast to this, the critical point CP(3,-1) between the cage carbon atoms in **9** is absent, in agreement with the considerable distortion of *closo* geometry in this complex which adopts a typical *pseudocloso* structure with a cage C(1)···C(2) separation of 2.418 Å.

AIM charges of C(1) and C(2) in **9** are more negative than in case of **6** (*ca.* 0.35 e, Table 4), while the charges of all carbon atoms of the η^5-Cp^* ligand and those of carbon atoms of the η^3-C_8H_{13} ligand that are directly coordinated by the Rh atom are nearly the same (−0.05 to −0.09 e). The positive charge of the cage boron atoms in both **6** and **9** depends on their positions in the carborane ligand. Those boron atoms which are directly attached to the cluster carbons C(1) and C(2) (e.g. B(4), B(5), B(11), B(7) and B(6) atoms) are more positive than other skeletal boron atoms. The least positively charged boron atoms are those positioned farthest away from either of the carbon atoms of the cage ligand, in particular B(9) and B(12). In general, the AIM positive charges of boron atoms in **9** are decreased compared to those located at the same position in complex **6**. The charges of H atoms of the carborane cage ligand both in **6** and **9** have very similar values, ranging from −0.48 to −0.52 e. Taking into account the observed distribution of AIM charges, one can conclude that the middle B_5-belt of the carborane polyhedron in **9**, as well as two boron atoms of its open face, B(4) and B(7), are substantially depleted in electron population compared with such boron positions in **6**. Thus, the valence electron density of carborane cage of **9**, which is actually localized in region of C(1) and C(2) atoms, can partially be donated to the Rh atom providing its stabilization.

Table 2
Calculated bond lengths in coordination polyhedron of Rh(III) in complexes **6** and **9**.

Bond length (Å)	**6**	**9**
C(1)–C(2)	1.735	2.439
Rh(3)–C(1)	2.187	2.129
Rh(3)–C(2)	2.187	2.214
Rh(3)–B(4)	2.174	2.229
Rh(3)–B(7)	2.170	2.217
Rh(3)–B(8)	2.171	2.126
Rh(3)–C(01)	2.260	2.202
Rh(3)–C(02)	2.166	2.146
Rh(3)–C(03)	2.170	2.243
Rh(3)–C(04)	2.216	
Rh(3)–C(05)	2.225	

Table 3
Topological characteristics of selected bonds in **6** and **9**.

Bond	Topological characteristics (a.u.)					
	6			**9**		
	$\rho(r)$	$\nabla^2\rho(r)$	$E^e(r)$	$\rho(r)$	$\nabla^2\rho(r)$	$E^e(r)$
C(1)–C(2)	0.1475	−0.1517	−0.1308			
Rh(3)–C(1)	0.0934	0.2251	−0.0365	0.1101	0.1718	−0.0583
Rh(3)–C(2)	0.0926	0.2252	−0.0357	0.0928	0.2078	−0.0373
Rh(3)–B(4)	0.0896	0.0457	−0.0477	0.0891	0.056	−0.019
Rh(3)–B(7)	0.0901	0.0459	−0.0482	0.0823	0.0665	−0.0391
Rh(3)–B(8)	0.0933	0.0292	−0.0527	0.0980	0.0134	−0.0610
Rh(3)–C(01)	0.0785	0.2340	−0.0218	0.0976	0.1818	−0.0442
Rh(3)–C(02)	0.0961	0.2077	−0.1331	0.0983	0.0983	−0.0405
Rh(3)–C(03)	0.0955	0.2091	−0.0399	0.0907	0.2071	−0.0353
Rh(3)–C(04)	0.0866	0.2322	−0.0293			
Rh(3)–C(05)	0.0850	0.2333	−0.0277			

Table 4
Selected AIM charges in **6** and **9**. The charges are calculated as difference between the population of atomic basin of the respective atoms and formal atomic number.

Atom	AIM charges (e)	
	6	**9**
Rh(3)	0.41	0.36
C(1)	−0.99	−1.49
C(2)	−1.01	−1.46
B(4)	0.70	0.79
B(5)	0.61	0.64
B(6)	0.80	0.91
B(7)	0.69	0.75
B(8)	0.58	0.55
B(9)	0.56	0.53
B(10)	0.59	0.51
B(11)	0.63	0.72
B(12)	0.50	0.51
C(01)	−0.08	−0.06
C(02)	−0.04	−0.05
C(03)	−0.06	−0.09
C(04)	−0.06	
C(05)	−0.06	

3. Conclusions

Two new examples of stable *pseudocloso*-type metallacarboranes with the η^3-cyclooctenyl ligand at the metal centers, [3-{(1–3-η^3)-C_8H_{13}}-1,2-$(PhCH_2)_2$-*pseudocloso*-3,1,2-$MC_2B_9H_9$] [**4**, M = Rh(III); **5**, M = Ir(III)] have been synthesized via simple room-temperature reaction between [K][7,8-$(PhCH_2)_2$-7,8-*nido*-$C_2B_9H_{10}$] and [(η^4-C_8H_{12})$_2$$M_2$($\mu$-Cl)$_2$] (M = Rh, Ir). The most remarkable peculiarity of both species **4** and **5** is that, despite their formally 16-electron structure, neither NMR spectroscopic (conventional for both **4** and **5**, and 2-D [^{1}H–^{1}H] NOESY/EXSY for **4**) nor crystallographic data could provide evidence supporting the presence of an agostic C–H···M bonding interaction in these compounds. The extraordinary stability of **4** and **5** is, therefore, associated with their cage-deformed cluster geometry, where electronically-deficient metal centers are believed to be stabilized by additional electron density released from the polyhedral C–C bond cleavage. DFT solid-state calculations on two model complexes: 18-electron [3-(η^5-C_5Me_5)-1,2-$(PhCH_2)_2$-*closo*-3,1,2-$RhC_2B_9H_9$] (**6**), and 16-electron [3-{(1–3-η^3)-C_8H_{13}}-1,2-(4′-$MeC_6H_4)_2$-*pseudocloso*-3,1,2-$RhC_2B_9H_9$] (**9**), showed that the AIM positive charges of boron atoms in complex **9** are decreased compared to those located at the same position in **6**, and charges of C(1) and C(2) in **9** are more negative than in case of **6**. This can reasonably be explained by partial donation of the carborane electron density in **9** to the Rh atom providing its stabilization.

4. Experimental

4.1. General comments

All reactions were carried out under an atmosphere of dry argon using standard Schlenk techniques. All solvents were dried over appropriate drying agents and distilled under an argon atmosphere prior to use. Starting reagents [K][7,8-$(PhCH_2)_2$-7,8-*nido*-$C_2B_9H_{10}$] (**1**) [20], [(η^4-C_8H_{12})$_2$$Rh_2$($\mu$-Cl)$_2$] (**2**) [21] and [($\eta^4$-$C_8H_{12}$)$_2$$Ir_2$($\mu$-Cl)$_2$] (**3**) [22] were prepared according to the literature methods. The room-temperature ^{1}H, ^{11}B, and ^{13}C{^{1}H} NMR spectra were obtained on a Bruker AMX-400 and Avance-600 instruments (*J* values are given in Hz). The 2D [^{1}H–^{1}H] NOESY/EXSY experiments were carried out on a Bruker AMX-400 at room temperature. IR spectra in KBr were recorded on a Bruker IFS-25 spectrometer. Elemental analyses were performed by the Analytical Laboratory of the Institute of Organoelement Compounds of the RAS.

4.2. Synthesis of [3-{(1–3-η^3)-C_8H_{13}}-1,2-$(CH_3)_2$-closo-3,1,2-$RhC_2B_9H_9$] (7) [23]

The salt [K][7,8-$(CH_3)_2$-7,8-*nido*-$C_2B_9H_{10}$] (0.048 g, 0.24 mmol) and the reagent **2** (0.050 g, 0.1 mmol) were dissolved in 10 ml of absolute benzene and stirred for 3 h. Then the solvent was removed *in vacuo* and the crude solid obtained was subjected to column chromatography using *n*-hexane-CH_2Cl_2 (1:1) as eluent. The broad red band was collected, the solvents removed to afford pure crystalline dark-red complex **7** (0.065 g, 87%). Anal. Calc. for $C_{12}H_{28}B_9Rh$: C, 38.69; H, 7.58; B, 26.11. Found: C, 38.91; H, 7.32; B, 26.26%. ^{1}H NMR (CD_2Cl_2, 400.13 MHz, *J* = *J*(H,H)): δ = 5.82 (2H, q, H(1), H(3), *J* = 8.4), 4.68 (1H, t, H(2), *J* = 7.6), 2.54 (2H, m, H(4-*exo*), H(8-*exo*)), 2.19 (6H, s, CH_3), 1.85 (3H, m, H(5-*exo*), H(6-*exo*), H(7-*exo*)), 1.75 (2H, m, H(5-*endo*), H(7-*endo*)), 1.44 (1H, m, H(6-*endo*)), 1.13 (2H, m, H(4-*endo*), H(8-*endo*)). ^{13}C{^{1}H} NMR (CD_2Cl_2; 100.61 MHz): δ = 104.10 (C(2)), 81.90 (C(1), C(3)), 30.80 (C(4), C(8)), 28.40 (C(5), C(7)), 26.50 (CH_3), 20.90 (C(6)). ^{11}B NMR (CD_2Cl_2, 128.33 MHz; *J* = *J*(B,H)): δ = 5.7 (1B, d, *J* = 146), -0.5 (1B, d, *J* = 142), −3.2 (2B, d, *J* = 154), −9.8 (2B, d, *J* = 140), −14.9 (3B, d, *J* = 158).

4.3. Synthesis of [3-{(1–3-η^3)-C_8H_{13}}-1,2-$(PhCH_2)_2$-pseudocloso-3,1,2-$RhC_2B_9H_9$] (4)

(a) To the salt **1** (0.050 g, 0.142 mmol) and the dimeric complex **2** (0.030 g, 0.061 mmol) taken as solids were added 8 ml of C_6H_6 and 2 ml of EtOH. The resulting homogeneous solution was stirred at room temperature for 4 h. Then the volatiles were removed under reduced pressure, the crude brown oily material thus obtained was dissolved in an eluent (CH_2Cl_2–*n*-hexane 1:1 mixture) and passed through silica gel chromatographic column using *n*-hexane–CH_2Cl_2 (1:1) as eluent. The resulting orange solid was recrystallized from *n*-hexane–CH_2Cl_2 mixture, affording analytically pure complex **4** (0.030 g, 47% yield). Anal. Calc. for $C_{24}H_{36}B_9Rh$: C, 54.93; H, 6.91; B, 18.54. Found: C, 54.90; H, 7.12; B, 18.44%. IR spectrum (ν_{max}/cm^{-1}): 2538 (BH). ^{1}H NMR (400.13 MHz, $CDCl_3$, *J* = *J*(H,H)): δ = 7.38–7.22 (10H, m, C_6H_5), 5.68 (2H, q, *J* = 8.5, H(1,3)), 4.74 (1H, t, H(2)), 4.16 (2H, d, J_{AB} = 15, C$H_2C_6H_5$), 3.65 (2H, d, J_{AB} = 15, C$H_2C_6H_5$), 2.47 (2H, m, H(4,8-*exo*)), 1.83 (3H, m, H(5,6,7-*exo*)), 1.73 (2H, m, H(5,7-*endo*)), 1.48 (1H, m, H(6-*endo*)), 1.08 (2H, H(4,8-*endo*)). ^{11}B NMR (128.33 MHz, $CDCl_3$, *J* = *J*(^{11}B,^{1}H)): δ = 10.8 (2B, d, *J* = 136), 10.2 (1B, d, *J* = 156), −2.0 (2B, d, *J* = 155), −6.8 (2B, d, *J* = 133), −7.7 (2B, d, *J* = 137), −20.5 (1B, d, *J* = 151).

(b) The salt **1** (0.050 g, 0.142 mmol) and the dimeric complex [(η^4-C_8H_{12})$_2$$Rh_2$($\mu$-Cl)$_2$] **2** (0.030 g, 0.061 mmol) were stirred in 10 ml of C_6H_6 at 60 °C. After 3 h the solution was allowed to cool to room temperature and the solvent was removed under reduced pressure. The crude solid material obtained was then purified by column chromatography on silica gel using *n*-hexane–CH_2Cl_2 (1:1) as eluent. The recrystallization of solid product from *n*-hexane overlayered CH_2Cl_2 solution afforded (0.060 g, 94%) of orange crystals, which from analysis of ^{1}H and ^{11}B{^{1}H} spectra was deduced to be complex **4**.

4.4. Synthesis of [3-{(1–3-η^3)-C_8H_{13}}-1,2-$(PhCH_2)_2$-pseudocloso-3,1,2-$IrC_2B_9H_9$] (5)

The salt **1** (0.040 g, 0.110 mmol) and the dimeric complex [(η^4-C_8H_{12})$_2$$Ir_2$($\mu$-Cl)$_2$] **3** (0.034 g, 0.051 mmol) were stirred in 12 ml of C_6H_6-EtOH (4:1) mixture for 3 h at ambient temperature. The reaction mixture was evaporated to dryness and the residue subjected to column chromatography on silica gel using *n*-hexane–CH_2Cl_2 (1:1) as eluent. The resulting orange solid was recrystallized from oxygen-free *n*-hexane–CH_2Cl_2 mixture under argon atmosphere, affording analytically pure complex **5** (0.060 g, 95%). IR spectrum (ν_{max}/cm^{-1}): 2536 (BH). Anal. Calc. for $C_{24}H_{36}B_9Ir$: C, 46.95; H, 5.86; B, 15.84. Found: C, 46.86; H, 5.91; B, 15.83%. ^{1}H NMR (400.13 MHz, CD_2Cl_2, −73 °C, *J* = *J*(H,H)): δ = 7.31 (4H, m, C_6H_5), 7.25 (2H, m, C_6H_5), 7.17 (4H, m, C_6H_5), 5.43 (1H, m, H(2)), 5.37 (2H, m, H(1,3)), 4.16 (2H, d, J_{AB} = 15.0, C$H_2C_6H_5$), 3.25 (2H, d, J_{AB} = 15.0, C$H_2C_6H_5$), 2.57 (2H, m, H(4,8-*exo*)), 1.86 (5H, m, H(5), H(6-*exo*), H(7)), 1.41 (1H, br d, J_{gem} = 15.8, H(6-*endo*)), 1.30 (2H, m, H(4-*endo*), H(8-*endo*)). ^{13}C{^{1}H} NMR (125.76 MHz, CD_2Cl_2, −30 °C): δ = 103.78 (C(2)), 100.71 (C(1,3)), 74.73 (C(carb.)), 50.97 ($CH_2C_6H_5$), 35.58 (C(4,8)), 31.68 (C(5, 7)), 23.03 (C(6)). ^{11}B NMR (128.33 MHz, $CDCl_3$, *J* = *J*(B,H)): δ = 13.8 (1B, d, *J* = 146), 11.1 (1B, d, *J* = 154), 1.8 (2B, d, *J* = 149), −4.1 (2B, d, *J* = 124), −6.3 (2B, d, *J* = 145), −22.9 (1B, d, *J* = 150).

4.5. Computational studies of complexes 6 and 9

The quantum chemical calculations of **6** and **9** in the crystal were carried out using the VASP 4.6.28 code [25]. Conjugated gradient technique was used for optimizations of the atomic positions (started from experimental data) and minimization of total energy. Projected augmented wave (PAW) method was applied to account for core electrons, while valence electrons were approximated by

Table 5
Crystal data, data collection and structure refinement parameters for **4** and **5**.

Complex	**4**	**5**
Formula	$C_{24}H_{36}B_9Rh$	$C_{24}H_{36}B_9Ir$
Molecular weight	524.73	614.02
Crystal color, habit	Orange prism	Orange prism
T (K)	120(2)	293(2)
Crystal system	Orthorhombic	Orthorhombic
Space group	$Pna2_1$	$Pna2_1$
a (Å)	16.5268(8)	16.656(5)
b (Å)	13.7846(7)	13.950(4)
c (Å)	22.3901(11)	22.521(6)
V ((Å^3)	5100.8(4)	5233(3)
Z	8	8
D_{calc} (g cm^{-3})	1.367	1.559
Diffractometer	SMART 1000 CCD	Enraf Nonius CAD4
Scan mode	ω	θ–5/3θ
θ_{max} (°)	29.0	30.0
μ (Mo Kα, λ = 0.71073 Å) (cm^{-1})	6.82	51.15
Absorption correction		ψ-Scan
Transmission factors, T_{min}/T_{max}	0.759/0.896	0.160/0.189
Number of unique reflections (R_{int})	12411 (0.0255)	8784 (0.0184)
Number of observed reflections ($I > 2\sigma(I)$)	10775	6241
Flack parameter	0.18(3)	0.25(1)
R_1 (on F for observed reflections)[a]	0.0397	0.0282
wR_2 (on F^2 for all reflections)[b]	0.0971	0.0695

[a] $R_1 = \Sigma||F_o| - |F_c||/\Sigma|F_o|$.
[b] $wR_2 = \{\sum[w(F_o^2 - F_c^2)^2]/\sum w(F_o^2)2\}^{1/2}$.

plane-wave expansion with 400 eV cutoffs [25]. Exchange and correlation terms of total energy were described by PBE [26] exchange–correlation functional. Kohn–Sham equations were integrated using Γ-point approximation. We believe that Γ-point approximation is sufficient for **6** and **9** because of their large crystal unit cells. Since it is not possible to take into account the dispersion interactions by the use of DFT method, the calculated cell parameters may be systematically overestimated or underestimated up to 5%. Thus, experimental values of the cell parameters were used in the calculations and at a final step atomic displacements converged were better than 0.02 eV Å^{-1}, and energy variations were less than 10^{-3} eV. In order to carry out the topological analysis of electron density distribution function in terms of R.F. Bader's theory "Atoms in molecules" (AIM) [18] the dense FFT (fast Fourier transformation) grid was used (corresponding to 1360 eV cutoff). The latter was obtained by a separate single point calculation of optimized geometry with the hard PAWs for each atom type. The topological analysis of electron density distribution function was carried out using AIM program – part of ABINIT software package [27].

4.6. Crystallographic studies of complexes *4* and *5*

Crystal data and the details of data collection and structure refinement parameters for complexes **4** and **5** are listed in Table 5. The structures were solved by direct methods and refined by the full-matrix least-squares technique against F^2 with the anisotropic temperature factors for all non-hydrogen atoms. Hydrogen atoms at the carborane ligands of **4** and **5** were located from the Fourier synthesis; the rest hydrogen atoms were placed geometrically. All hydrogen atoms were included in the structure factors calculations in the riding motion approximation. SHELXTL-97 [28] program package was used throughout the calculations.

Acknowledgements

The financial support of this study is provided by the Russian Foundation of Basic Research (Grant Nos. 06-03-32172 and 07-03-00631), and the Program of Basic Research of the Chemistry and Materials Science Division of the RAS.

Appendix A. Supplementary material

CCDC 693865 and 693866 contains the supplementary crystallographic data for **4** and **5**. These data can be obtained free of charge from The Cambridge Crystallographic Data Center via http://www.ccdc.cam.ac.uk/data_request/cif. Supplementary data associated with this article can be found, in the online version, at doi:10.1016/j.jorganchem.2009.01.014.

References

[1] Z.G. Lewis, A.J. Welch, J. Organomet. Chem. 430 (1992) C45.
[2] R.L. Tomas, G.M. Rosair, A.J. Welch, Chem. Commun. (1996) 1327.
[3] A.J. Welch, Steric effects in metallacarboranes, in: P. Braunstein, L.A. Oro, P.R. Raithby (Eds.), Metal Clusters in Chemistry, Wiley-VCH, Weinheim, 1999, p. 26 (a review).
[4] (a) M.A. McWhannel, G.M. Rosair, A.J. Welch, F. Teixidor, C. Viñas, J. Organomet. Chem. 573 (1999) 165;
(b) G. Barbera, S. Dunn, M. Fox, R.M. Garrioch, B.E. Hodson, K.S. Low, G.M. Rosair, F. Teixidor, C. Viñas, A.J. Welch, A.S. Weller, in: M.G. Davidson, A.K. Hughes, T.B. Marder, K. Wade (Eds.), Contemporary Boron Chemistry, Royal Society of Chemistry, Cambridge, UK, 2000, p. 329;
(c) F. Teixidor, C. Viñas, M.A. Flores, G.M. Rosair, A.J. Welch, A.S. Weller, Inorg. Chem. 37 (1998) 5394;
(d) R.M. Garrioch, G.M. Rosair, A.J. Welch, J. Organomet. Chem. 614–615 (2000) 153;
(e) J. Llop, C. Viñas, F. Teixidor, L. Victori, R. Kivekäs, R. Sillanpää, Organometallics 20 (2001) 4024;
(f) A.V. Safronov, F.M. Dolgushin, P.V. Petrovskii, I.T. Chizhevsky, Organometallics 24 (2005) 2964;
(g) R.D. McIntosh, D.E. Ellis, B.T. Giles, S.A. Macgregor, G.M. Rosair, A.J. Welch, Inorg. Chim. Acta 359 (2006) 3745.
[5] L.S. Alekseev, F.M. Dolgushin, I.T. Chizhevsky, J. Organomet. Chem. 693 (2008) 3331.
[6] L.S. Alekseev, F.M. Dolgushin, A.S. Korlukov, I.A. Godovikov, E.V. Vorontsov, I.T. Chizhevsky, Organometallics 26 (2007) 3868.
[7] (a) T.V. Zinevich, A.V. Safronov, E.V. Vorontsov, P.V. Petrovskii, I.T. Chizhevsky, Russ. Chem. Bull. 50 (2001) 1702 [Izv. Akad. Nauk, Ser. Khim. (2001) 1620];
(b) A.V. Safronov, T.V. Zinevich, F.M. Dolgushin, E.V. Vorontsov, O.L. Tok, I.T. Chizhevsky, Russ. Chem. Bull. 50 (2001) 2254 [Izv. Akad. Nauk, Ser. Khim. (2001) 2152];
(c) A.V. Safronov, M.N. Sokolova, E.V. Vorontsov, P.V. Petrovskii, I.G. Barakovskaya, I.T. Chizhevsky, Russ. Chem. Bull. 53 (2004) 1875 [Izv. Akad. Nauk, Ser. Khim. (2004) 1875].
[8] W.-C. Kwong, H.-S. Chan, Y. Tang, Z. Xie, Organometallics 23 (2004) 4301.
[9] (a) Z. Xie, Z. Liu, K.-y. Chiu, F. Xue, T.C.W. Mak, Organometallics 16 (1997) 2460;
(b) Z. Xie, Z. Liu, Q. Yang, T.C.W. Mak, Organometallics 18 (1999) 3603.
[10] (a) R.K. Brown, J.M. Williams, A.J. Schultz, G.D. Stucky, S.D. Ittel, R.L. Harlow, J. Am. Chem. Soc. 102 (1980) 981;
(b) T.V. Ashworth, D.C. Liles, E. Singleton, Organometallics 3 (1984) 1851;
(c) B.E. Hodson, T.D. McGrath, F.G.A. Stone, Organometallics 24 (2005) 1638.
[11] D.M. Speckman, C.B. Knobler, M.F. Hawthorne, Organometallics 4 (1985) 426.
[12] F. Teixidor, M.A. Flores, C. Viñas, R. Sillanpää, R. Kivekäs, J. Am. Chem. Soc. 122 (2000) 1963.
[13] A.V. Safronov, T.V. Zinevich, F.M. Dolgushin, O.L. Tok, E.V. Vorontsov, I.T. Chizhevsky, Organometallics 23 (2004) 4970.
[14] A.V. Safronov, T.V. Zinevich, F.M. Dolgushin, E.V. Vorontsov, O.L. Tok, I.T. Chizhevsky, J. Organomet. Chem. 680 (2003) 111.
[15] The choice of solid-state quantum chemical calculation rather than a gas phase study of isolated molecules was dictated by necessity to reproduce the crystal packing features of structures **6** and **9**. Actually, in their crystal structures some distances C···H and H···H between phenyl and methylene groups are less than sum of Van-der-Waals radii of the above atoms (2.42 and 3.02 Å [16,17]) that can be interpreted as the presence of repulsive interactions between these groups (e.g. the interatomic distance C(20)···H(14) in crystal of **9** and H···H in **6** are equal to 2.77 and 2.12 Å, respectively). Consequently, one may propose that the mutual orientation of phenyl groups will be changed in the absence of the crystal packing and the separation of C(1) and C(2) atoms in the will be increased compared with their crystal structures. Indeed our preliminary calculations of isolated molecules of **6** and **9** using PC-GAMESS program have shown that the differences between the calculated isolated molecules and experimental C···C distance in **6** is 0.07 Å while in **9** it is 0.21 Å, e.g. the former ones are considerably larger than those in the crystals.
[16] R.S. Rowland, R. Taylor, Phys Chem. 100 (1996) 7384.
[17] A. Bondi, J. Phys. Chem. 68 (1964) 441.
[18] R.F.W. Bader, Atoms in Molecules. A Quantum Theory, Clarendron Press, Oxford, 1990.
[19] I.V. Glukhov, K.A. Lyssenko, A.A. Korlyukov, M.Yu. Antipin, Faraday Discuss. 135 (2007) 203.
[20] Z. Xie, Z. Liu, K.-Y. Chiu, F. Xue, T.C.W. Mak, Organometallics 16 (1997) 2460.
[21] G. Giordane, R.H. Crabtree, Inorg. Synth. 28 (1979) 88.
[22] R.H. Crabtree, J.M. Quirk, Synth. React. Inorg. Met.-Org. Chem. 12 (1982) 407.

[23] The synthesis of **7** can also be carried out either in C_6H_6–EtOH (4:1) mixture [7a] or in CH_2Cl_2 [24].
[24] A.R. Kudinov, R.T. Bogoudinov, P.V. Petrovskii, M.I. Rybinskaya, Russ. Chem. Bull. 3 (1999) 586 [Izv. Akad. Nauk, Ser. Khim. (1999) 592].
[25] (a) G. Kresse, J. Hafner, Phys. Rev. B47 (1993) 558;
(b) G. Kresse, Thesis, Technische Universitat Wien, 1993.;
(c) G. Kresse, J. Furthmuller, Comput. Mater. Sci. 6 (1996) 15;
(d) G. Kresse, J. Furthmuller, Phys. Rev. B54 (1996) 11169.
[26] J.P. Perdew, S. Burke, M. Ernzerhopf, Phys. Rev. Let. 77 (1996) 3865.
[27] X. Gonze, J.-M. Beuken, R. Caracas, F. Detraux, M. Fuchs, G.-M. Rignanese, L. Sindic, M. Verstraete, G. Zerah, F. Jollet, M. Torrent, A. Roy, M. Mikami, P. Ghosez, J.-Y. Raty, D.C. Allan, Comput. Mater. Sci. 25 (2002) 478.
[28] G.M. Sheldrick, SHELXTL-97 V5.10, Bruker AXS Inc., Madison, WI-53719, USA, 1997.